An X-ray absorption spectroscopy study of the pressure and temperature dependence of $ZnBr_2$ aqueous supercritical solutions

Y. Calzavara,[a] V. Simonet,[b] J. L. Hazemann,[c] R. Argoud,[a] O. Geaymond[a] and D. Raoux[a]*

[a]Laboratoire de Cristallographie, CNRS and Université J. Fourier, 25 Av. des Martyrs, Grenoble 38042, CEDEX 9, France, [b]Laboratoire de Physique des Solides, Université d'Orsay and CNRS, Orsay, France, and [c]LGIT, Université J. Fourier and CNRS, Domaine Universitaire, Saint Martin d'Hères, France. E-mail: draoux@polycnrs-gre.fr

X-ray absorption spectroscopy (XAS) experiments have been performed on 1.0 and 1.6 *M* $ZnBr_2$ aqueous solutions under ambient to supercritical conditions. Both the X-ray absorption near-edge structure (XANES) and the extended X-ray absorption fine structure (EXAFS) show striking evolutions, which indicate major structural changes, with a strong reduction in hydration and the increasing formation of ZnBr pairs. A quantitative analysis of the evolution of the Zn environment is presented that supports the existence of a transition from an octahedral to a tetrahedral environment.

Keywords: zinc bromide; supercritical solutions; phase transitions; pressure/temperature dependence.

1. Introduction

The very peculiar properties of supercritical fluids have recently attracted much interest because of their importance in Earth science, as well as their use in several types of industrial processes, such as extraction and synthesis. In the environmental field, they are used for chemical decomposition of hazardous organic wastes. At temperatures and pressures greater than critical ones (647.1 K and 221 bar for water; 1 bar = 10^5 Pa), a fluid undergoes a continuous transition from liquid to gas phase, with huge changes in its density, isothermal compressibility and thermal conductivity, whereas a very low viscosity is observed. Additionally, polar fluids like water undergo an important decrease in their dielectric constant (from about 80 under ambient conditions to 2 at 720 K in the case of water), which leads to drastic modifications of their solvating power. The solvation screening of the electric charges of ions in aqueous solutions diminishes, which eventually leads to ion-pair formation, complexation and, ultimately, salt precipitation. These properties might offer new possibilities for depollution, such as extraction of toxic inorganic salts present in water or in waste residues.

The present work is aimed at investigating the changes in the local structure occurring in $ZnBr_2$ aqueous solutions under supercritical conditions. In a first step, our attention was drawn towards zinc since it is one of the major toxic pollutants (Nriagu & Pacyna, 1988) and since its X-ray *K*-absorption edge at 9659 eV can easily be probed by XAS. Water has been chosen as a polar solvent as it is ubiquitous in nature. Finally, in order to observe solvation and ion pairing selectively, bromine was selected as a counter-ion since its contribution to EXAFS spectra can be rather easily separated from that of oxygen neighbours. In fact, there have already been XAS investigations of $ZnCl_2$ (Mayanovic *et al.*, 1999) and $NiBr_2$ aqueous solutions (Wallen *et al.*, 1997, 1998; Hoffman *et al.*, 1999) under sub- or supercritical conditions. They show similarities, but also discrepancies which may arise from the different types of investigated ions, but also from the different salt concentrations or pressure and temperature paths employed. They partly motivate this work, which aims at clarifying the respective influences of these parameters, especially those of pressure and temperature, which can be independently varied thanks to our specific experimental setup.

In this paper, we focus on the drastic changes occurring in the Zn environment in 1.0 and 1.6 *M* $ZnBr_2$ solutions, between ambient conditions and supercritical ones. The changes are evidenced by the evolution of the Zn *K*-edge XAS spectra, both in the XANES and in the EXAFS ranges. XAS transmission measurements have been performed at fixed pressure (250 bar) with the temperature varied up to about 650 K in the case of the 1.0 *M* solution, and at two fixed temperatures (room temperature and 570 K) with the pressure varied up to 2000 bar in the case of the 1.6 *M* solution. Similar measurements have also been performed recently at the Br *K* edge at a weaker concentration of 0.1 *M*. The results will be reported in a forthcoming paper (Simonet *et al.*, 2001). In all cases, there is no evidence of precipitation under sub- or supercritical conditions. Clear changes are, however, observed in the XANES and EXAFS spectra at both the Zn edge and the Br edge with increasing temperature, up to supercritical conditions. On the other hand, we do not observe a strong pressure dependence up to 2000 bar, neither at room temperature nor at 570 K. This is not that surprising since density dramatically decreases with temperature, but does not change much with pressure.

2. Experimental conditions and data analysis

The solutions were prepared by dissolving high-purity anhydrous $ZnBr_2$ powder in deionized water. They were pre-filled inside a polycrystalline alumina cell, which does not react with supercritical water. The cell, especially designed for the study of fluids under extreme conditions, has been described in detail elsewhere (Tamura *et al.*, 1995). It consists of a sample chamber heated by a molybdenum oven and is connected to a cooler reservoir. Temperatures near the cell and the reservoir are measured by potassium thermocouples and controlled within 0.1 K. Thermal shields around the sample cell insure that the temperature gradient is lower than 1 K along the cell. The cell is inserted inside a high-pressure steel vessel, with two Be windows, of 5 mm thickness, on the X ray beam path. The whole vessel is pressurized with helium gas. This setup allows independent variation of the pressure and temperature up to about 2000 bar and 2000 K, respectively (Soldo *et al.*, 1998).

The measurements were performed using the spectrometer installed by the French Collaborative Research Group on the BM32 beamline on a bending magnet at the ESRF. The beamline setup includes a vertically focusing platinum-coated mirror and an Si (111) sagitally focusing double-crystal monochromator (Hazemann *et al.*, 1995), which provide a 0.2 × 0.2 mm X-ray beam with 10^{12} photons. Dynamical focusing keeps the focus position fixed throughout an EXAFS scan. Silicon diode detectors located before and after the sample are used to measure the X-ray intensities scattered by kapton foils in the beam path.

The EXAFS oscillations were analysed within the single-scattering approximation, using the *SEDEM* package (Aberdam, 1998). This package allows an estimation of the uncertainties in the determination of the structural parameters N, R and σ, by taking into account the effects of correlation between these parameters, as well as those of statistical noise in the data. For each EXAFS spectrum, the noise figure is estimated from the inverse Fourier spectrum of the pseudo radial distribution function, calculated at R values larger than any

Table 1
Zn–O and Zn–Br coordination numbers *N*, pair distances *R* and Debye–Waller factors σ^2 obtained from the simulations of the XAFS spectra.

Parameter values are presented for a 1 *M* $ZnBr_2$ solution at 250 bar at various temperatures. The values of the parameters for solid $Zn(NO_3)_2.6H_2O$ and solid $ZnBr_2$ reference materials are also given for comparison. Standard uncertainties are given within parentheses.

		1 *M* $ZnBr_2$ solution at 250 bar				
	$Zn(NO_3)_2.6H_2O$	303 K	373 K	473 K	573 K	Solid $ZnBr_2$
N_{H_2O}	6.00 (2)	5.3 (4)	4.1 (2)	2.9 (2)	2.4 (1)	
R_{H_2O} (Å)	2.096 (3)	2.087 (4)	2.064 (6)	2.026 (6)	2.006 (6)	
$\sigma^2_{H_2O}$ (10^{-3} Å^2)	6.30 (4)	9.9 (6)	12.0 (14)	11 (1)	9 (1)	
N_{Br}		1.1 (8)	2.1 (4)	2.4 (3)	2.1 (3)	4.0 (2)
R_{Br} (Å)		2.38 (1)	2.369 (8)	2.349 (6)	2.328 (6)	2.403 (3)
σ^2_{Br} (10^{-3} Å^2)		10 (3)	10 (1)	10 (1)	10.0 (9)	6.5 (4)

interatomic distance. The *SEDEM* package also allows the harmonic approximation to be exceeded by using the cumulant method by decorrelating the phase and amplitude for a single shell. The Zn–O and Zn–Br backscattering amplitudes and phase shifts were extracted from $Zn(NO_3)_2.6H_2O$ and $ZnBr_2$ reference spectra, respectively. $Zn(NO_3)_2.6H_2O$ was selected since Zn atoms are surrounded by an octahedron of oxygen neighbours as in dilute Zn solutions. In $ZnBr_2$, Zn atoms are located at the centres of tetrahedra of Br neighbours. Simulations of the Zn-edge XANES were performed using the *FDMNES* package (Joly, 1997) using either the multiple-scattering approach or the finite difference method. Both yielded very similar simulations for all samples investigated in this work.

3. The local structure around Zn atoms

3.1. *Qualitative evidence for dehydration and ion pairing in the supercritical regime*

Fig. 1 shows the inverse Fourier filtered transforms of EXAFS spectra measured at the Zn *K* edge for a 1.6 *M* solution, at room temperature and at 570 K. Fig. 2 shows the real and imaginary parts of their Fourier transforms. The corresponding XANES spectra are displayed in Fig. 3, together with those for a dilute 0.0062 *M* $ZnSO_4$ solution and for crystalline $ZnBr_2$. A striking evolution is observed between ambient and supercritical conditions, with a large decrease in the white-line intensity and a change in the absorption edge shape. At room temperature, the intensity of the white line is very similar to that found for very dilute solutions, suggesting an octahedral oxygen environment. Its decrease with increasing temperature indicates a decrease in the Zn hydration. This is also supported by the shift of the threshold energy by 0.7 eV towards smaller values between room temperature and 650 K. Moreover, in spectra measured at temperatures below 470 K, a weak oscillation is seen around 9680 eV on the higher energy side of the white line, which disappears at higher temperatures. Such a feature is also found in the spectra of very dilute Zn solutions, where it has been attributed to multiple-scattering effects produced by the octahedral environment formed by water molecules (Kuzmin *et al.*, 1997). Its decrease suggests a marked reduction in the octahedral environment of Zn atoms at temperatures higher than 470 K. Beyond that temperature, the XANES shape looks similar to that of solid $ZnBr_2$, with a frequency beat around 50 eV caused by interference between the contributions from O and Br backscatterers. This suggests that local environments of Zn atoms similar to the tetrahedral ones found in crystalline $ZnBr_2$ salt are formed when approaching critical conditions. The Br-edge spectra show a similar trend from room temperature to 650 K, their shapes evolving from that of a very dilute Br solution to that of crystalline $ZnBr_2$ (Simonet *et al.*, 2001).

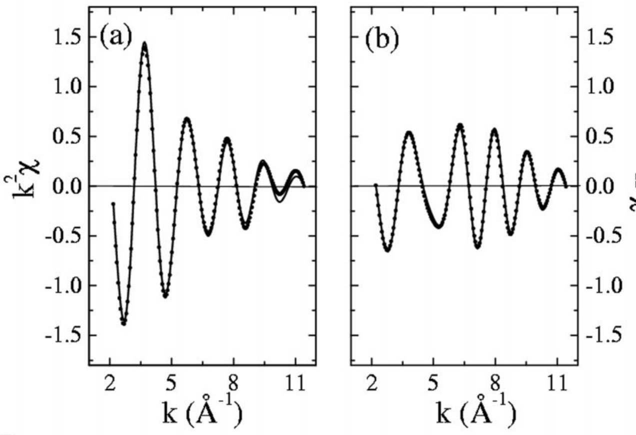

Figure 1
Filtered $k^2\chi(k)$ for a 1 *M* $ZnBr_2$ aqueous solution at 303 K and 250 bar (*a*), and at 573 K and 250 bar (*b*). The experimental spectra (circles) are compared with simulations (lines), from which the parameter values listed in Table 1 were obtained.

The filtered EXAFS spectra shown in Fig. 1 also support such an evolution. At ambient conditions (Fig. 1*a*), they look like that of diluted solutions, with decreasing oscillations that can be attributed to oxygen neighbours. With increasing temperature, their amplitudes decrease at low *k* values as shown in Fig. 1(*b*), supporting the assumption of a decrease in the Zn hydration. Beyond $k = 3.5$ Å^{-1}, the oscillations shift towards higher *k* values as a result of the Br contribution at a shorter interatomic distance. This evolution is more clearly seen in the Fourier transforms shown in Fig. 2. At 570 K (Fig. 2*b*), two coordination shells are displayed that correspond to Zn–O and Zn–Br pairs. At room temperature (Fig. 2*a*), the amplitude of the Zn–O main peak at 1.6 Å is much larger. A weak Br contribution is, however, evidenced on its large-distance side with an interference effect in the real part of the Fourier transform. Similar but even larger changes are observed at the Br edge for the more dilute 0.1 *M* solution. In that case, the EXAFS spectra do not seem to show any Zn–Br bonding contribution at room temperature.

3.2. *Quantitative results*

The quantitative analysis of the EXAFS spectra at the Zn edge has been performed using the harmonic approximation and assuming a mixing of both O and Br sub-shells. The simulations obtained both in *k* and in *r* space are compared with experimental data in Figs. 1 and 2. The values of the corresponding pair distances, *R*, coordination numbers, *N*, and Debye–Waller factors, σ, are listed in Table 1. The σ values for Zn–O bonds are the same as in very dilute solutions, where Zn ions are in an octahedral highly solvated environment. However, their values, as well as those for Zn–Br, are larger than those found for the crystalline reference materials. The use of the harmonic approximation may then be questioned. Actually, the use of the cumulant approximation is difficult because the two Zn–O and Zn–Br shells cannot be isolated by Fourier filtering and the limited available *k* range does not allow extraction of more than eight independent parameters. It can, however, be safely used in the case of very dilute 0.0044 *M* $ZnBr_2$ solutions where no Zn–Br ion pairing occurs and where the $\sigma = 0.098$ Å value for Zn–O bonds is similar to those for the 1.0 and 1.6 *M* solutions. In that case, we checked that the use of the cumulant approximation up to the fourth or sixth order does not change the *R* and *N* values. Similar conclusions can thus be derived for Zn–O bonds in the 1.0 and 1.6 *M* solutions. For Zn–Br bonds, the use of cumulants up to the fourth order very slightly increases the Zn–Br distances, by less than 0.005 Å. It does not change the coordination numbers, within the uncertainties quoted in Table 1. This validates the use of the harmonic approximation, which restricts the number of free parameters in the simulations. Moreover, the Zn–O and Zn–Br σ values for the 1.0 and 1.6 *M* solutions do not change much when varying temperature, which implies coherence between results at various temperatures.

As seen in Table 1, the number of oxygen neighbours in the 1.0 *M* solution decreases from 5.3 (4) at 303 K to 2.4 (1) under supercritical conditions, demonstrating a dramatic reduction in the hydration of Zn^{2+} ions. The same effect is found for the 1.6 *M* solution. A clear contraction of the hydration sphere is also observed with a shortening of Zn–O distances from 2.087 to 2.006 (6) Å, without any noticeable variation in σ values. Because of the high salt concentration, there are already Zn–Br ion pairs at room temperature, with a Br coordination number around 1.1 (8) at 1.0 *M* and 1.3 (5) at 1.6 *M*. At 473 K, the number of Br neighbours increases to about 2.4 (3) for a 1.0 *M* solution and to 2.3 (1) for a 1.6 *M* solution, showing a very weak concentration dependence, if any. It does not seem to vary significantly at higher temperatures. As a result, a continuous decrease in the Zn total coordination number from 6 to 4 occurs between room temperature and 573 K. The Zn–Br distance slightly decreases from 2.38 (1) to 2.328 (6) Å from 303 to 573 K, while σ does not significantly change. This shortening in the Zn–Br distance suggests a strengthening of the ion-pair bonding.

4. Discussion

All three sets of XAS results at 1.0 and 1.6 *M* evidence the same structural evolution from ambient to supercritical conditions. Actually, the total Zn coordination number, as well as the partial O and Br coordination numbers and the interatomic distances, can all be plotted *versus* water density, which seems to be the pertinent parameter, instead of temperature and pressure. Preliminary analysis of Br-edge XAS spectra of 0.1 and 1.0 *M* solutions also shows the same trend. First, a strong decrease of the Zn hydration is observed. This is in agreement with the few previously published XAS and neutron scattering studies of supercritical aqueous solutions (Yamaguchi *et al.*, 1996; Sewards *et al.*, 1996; Jong *et al.*, 1996; Fulton *et al.*, 1996; Wallen *et al.*, 1997, 1998; Hoffmann *et al.*, 1999). Second, a concomitant formation of well defined Zn–Br structures and a transition in the Zn environment from six- to four-coordination is found. At ambient conditions, the main species is the $Zn(H_2O)_6$ sixfold-hydrated cation. Both the value of the Zn–O distance, 2.09 Å, and the XANES shape indicate an octahedral environment of water molecules, as is the case in dilute solutions. There is, however, already some ion pairing because of the high salt concentration. EXAFS at the Br edge suggests that this is not the case for more dilute 0.1 *M* solutions. Between room temperature and 300–470 K, the number of Br neighbours around Zn cations increases up to about two and stays roughly stable up to the highest investigated temperature, 650 K. Meanwhile, the Zn–O coordination number continuously decreases from 6 to 2. Indeed, the final state beyond 570 K is compatible with the existence of hydrated complexes including on average one Zn^{2+}, two Br^- ions and two water molecules. The decrease in Zn–O distance from 2.09 to 2.00 Å from room temperature to 620 K suggests an evolution from an octahedral O environment to a tetrahedral one. Under supercritical conditions, the similarities between the XANES spectra and those of crystalline $ZnBr_2$, at both the Zn edge and the Br edge, also support a tetrahedral environment around Zn ions. Simulations of the Zn-edge XANES suggest that the Zn environment could mainly result from a mixture of tetrahedral $Zn(H_2O)_4$ and $ZnBr_4$ species with temperature-dependent proportions. Neutral $ZnBr_2(H_2O)_2$ complexes, which could be favoured in supercritical conditions because of the low value of the dielectric constant, actually yield a different XANES shape. Therefore, though they cannot be excluded, they should not occur in large concentrations. Finally, the shortening of Zn–Br pair distances with increasing temperature from room temperature to supercritical ones, indicates a strengthening of the bonding of Zn ions to Br neighbours that is, in our opinion, directly related to the decrease in the dielectric constant.

Finally, we compare our EXAFS findings with those recently published for $ZnCl_2$ (Mayanovic *et al.*, 1999) and $NiBr_2$ (Hoffmann *et*

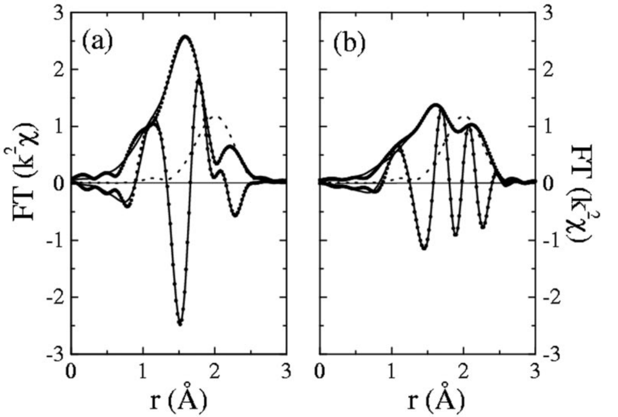

Figure 2
Real and imaginary parts of the Fourier transform of $k^2\chi(k)$ for a 1 *M* $ZnBr_2$ aqueous solution at 303 K and 250 bar (*a*), and at 573 K and 250 bar (*b*). The experimental spectra (circles) are compared with simulations (full lines), from which the parameter values listed in Table 1 were obtained. The contribution of the Br shell to the modulus of the Fourier transform is also shown as a dotted line.

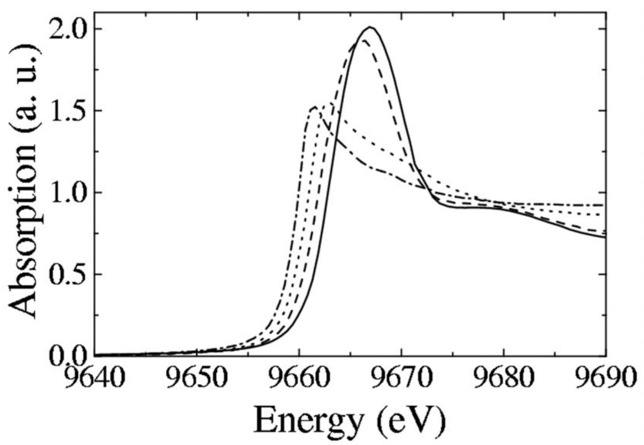

Figure 3
Zn *K*-edge XANES spectra for a 1 *M* $ZnBr_2$ aqueous solution at 250 bar and at two temperatures: 303 (dashed line) and 573 K (dotted line). The spectra at 303 K for solid $ZnBr_2$ (dash-dotted line) and for a 0.0062 *M* $ZnSO_4$ solution (full line) are also shown for comparison.

al., 1999) solutions. In all cases, the average environment of the Zn (Ni) cation is found to include two O and two Cl or Br neighbours under supercritical conditions. Our results mostly agree with those found for 0.2 *M* $NiBr_2$ solutions (Hoffmann *et al.*, 1999) which show a similar trend towards dehydration and towards a transition in the structure around the Ni cations from six- to four-coordinate upon formation of ion pairs. However, for 2 *M* $ZnCl_2$ solutions (Mayanovic *et al.*, 1999), no change was observed in the tetrahedral local structure around Zn cations from the vapour phase at ambient conditions to the supercritical state. The origin of such a difference is not clear up to now. Concentration effects do not seem to explain it, since we did not observe significant differences in the behaviour of 1.0 and 1.6 *M* solutions.

References

Aberdam, D. (1998). *J. Synchrotron Rad.* **5**, 1287–1297. (See also http://www.esrf.Fr/computing/expg/subgroups/theory/xafs/aberdam.html.)

Fulton, J. L., Pfund, D. M., Wallen, S. L., Newville, M., Stern, E. A. & Ma, Y. (1996). *J. Chem. Phys.* **105**, 2161–2166.

Hazemann, J. L., Nayouf, K. & de Bergevin, F. (1995). *Nucl. Instrum. Methods B*, **97**, 547–550.

Hoffmann, M. M., Darab, J. G., Palmer, B. J. & Fulton, J. L. (1999). *J. Phys. Chem. A*, **103**, 8471–8482.

Joly, Y. (1997). *J. Phys. IV Fr.* **7**(C2), 111–115.

Jong, P. H. K., Neilson, G. W. & Bellisent-Funel, M.-C. (1996). *J. Chem. Phys.* **105**, 5155–5159.

Kuzmin, A., Obst, S. & Purans, J. (1997). *J. Phys. Condens. Matter*, **9**, 10065–10069.

Nriagu, J. O. & Pacyna, J. M. (1988). *Nature (London)*, **333**, 134–139.

Mayanovic, R. A., Anderson, A. J., Bassett, W. A. & Chou, I. M. (1999). *J. Synchrotron Rad.* **6**, 195–197.

Sewards, T. M., Henderson, C. M. B., Charnock, J. M. & Dobson, B. R. (1996). *Geochim. Cosmochim. Acta*, **60**, 2273–2282.

Simonet, V., Calzavara, Y., Hazemann, J. L. & Raoux, D. (2001). To be submitted.

Soldo, Y., Hazemann, J. L., Aberdam, D., Inui, M., Tamura, K., Raoux, D., Pernot, E., Jal, J. F. & Dupuy-Philon, J. (1998). *Phys. Rev. B*, **57**, 258–268.

Tamura, K., Inui, M. & Hosokawa, S. (1995). *Rev. Sci. Instrum.* **62**, 1382.

Wallen, S. L., Palmer, B. J. & Fulton, J. L. (1998). *J. Chem. Phys.* **108**, 4039–4046.

Wallen, S. L., Palmer, B. J., Pfund, D. M. & Fulton, J. L. (1997). *J. Phys. Chem. A*, **101**, 9632–9640.

Yamaguchi, T., Yamagami, M., Ohzono, H., Wakita, H. & Yamanaka, K. (1996). *Chem. Phys. Lett.* **252**, 317–321.

Received 31 July 2000 • Accepted 28 November 2000